Available online at website: https://journal.bcrec.id/index.php/bcrec

Bulletin of Chemical Reaction Engineering & Catalysis, 21 (1) 2026, 1-10

Original Research Article

One Pot Synthesis of N-acetylglycine from N-acetyl Glucosamine over Bifunctional Ag/MgO

Dianwen Qi[1], Qingya Cao*[1,2], Chenxi Huang[1], Xueying Qi[1], Chongzhou Wang[1], Jinhang Dai*[1]

[1]School of Environment and Resources, Chongqing Technology and Business University, Chongqing 400067, P. R. China
[2]Chongqing Sanxia Paints Company Limited, Chongqing 402284, P. R. China.

Received: 6th September 2025; Revised: 26th October 2025; Accepted: 27th October 2025
Available online: 2th November 2025; Published regularly: April 2026

Abstract

The catalytic conversion of chitin biomass provides an environment-friendly approach for the synthesis of valuable organonitrogen compounds. Here, we prepared bifunctional Ag/MgO by simple deposition-precipitation method. The catalysts exhibited good catalytic activity for one pot synthesis of N-acetylglycine (AcGly) from N-acetyl glucosamine (NAG), offering a 26.2% yield under optimized conditions. The basic nature of MgO contributed to the retro-aldol of NAG, and Ag species catalyzed the oxidation of intermediate to AcGly. The spent catalyst could be recycled and reused for NAG conversion to AcGly.

Keywords: Chitin; N-acetylglycine; Bifunctional; Retro-aldol; Oxidation

How to Cite: Qi, D., Cao, Q., Huang, C., Qi, X., Wang, C., Dai, J. (2026). One Pot Synthesis of N-acetylglycine from N-acetyl Glucosamine over Bifunctional Ag/MgO. *Bulletin of Chemical Reaction Engineering & Catalysis*, 21 (1), 1-10. (doi: 10.9767/bcrec.20482)

Permalink/DOI: https://doi.org/10.9767/bcrec.20482

1. Introduction

Currently, fossil resources are playing significant roles in most fields such as transportation, materials, chemistry industry, and so on. Nevertheless, fossil resources are limited and non-renewable. It is of significance to find renewable and abundant resource to replace fossil resources. The biomass has been regarded as the best candidate. Lignin, cellulose, hemicellulose, and chitin are typical bio-polymers that can be used for producing chemicals and fuels [1-8]. Among them, chitin is special because it contains bio-fixed nitrogen. A significant concept of "Shell biorefinery" has been proposed, which promoted investigations on chitin biomass (referring to chitin and its derivatives) utilization [9-13].

Typically, the conversion of chitin biomass is a novel strategy to produce nitrogen-containing chemicals, which avoids the use of additional nitrogen source (i.e., ammonia gas, a compound produced via energy-intensive process). The hydrolysis of chitin or chitosan produces oligosaccharides or monosaccharides [14-16], such as N-acetyl glucosamine (NAG) and glucosamine. The dehydration of NAG offers 3-acetamido-5-acetylfuran (3A5AF) [17-21], a furan-derived platform compound. A few valuable chemicals have been produced from 3A5AF [22-25]. Moreover, some amino acids [26-29] and amino alcohols [30] can be prepared by simple oxidation and reduction of NAG or glucosamine, respectively.

Precise cleavage of C-C bond in chitin biomass provides opportunity to prepare small nitrogen-containing chemicals [29,31]. For example, Fukuoka and coworkers [29] reported the synthesis of N-acetylmonoethanolamine (NMEA) from NAG by successive retro-aldol and hydrogenation over Ru/C and $NaHCO_3$ in H_2.

* Corresponding Author.
Email: caoqingya1125@163.com (Q. Cao);
jinhangdai@ctbu.edu.cn (J. Dai)

After changing H_2 to O_2, NMEA could be transformed into N-acetylglycine (AcGly) by oxidation, as shown in Figure 1a. AcGly is a useful amino acid derivative and can be applied in the fields of medicine [32,33], catalysis [34,35], and optical materials [36]. Fukuoka's work proposed a new strategy for green synthesis of AcGly, avoiding the use of toxic reactants such as hydrogen cyanide and formaldehyde in traditional methods. However, the low overall yield of 6% is unsatisfactory. To improve AcGly yield, our group [27] tried the oxidation of NMEA by O_2 using $Fe(NO_3)_3.9H_2O$, TEMPO and KCl, and a 63% of AcGly yield was obtained. And one pot synthesis of AcGly from NAG via successive retro-aldol and oxidation was achieved, in which Ag_2O and MgO acted as oxidation and retro-aldol catalysts, respectively. A boosted yield of 29.4% was obtained [37], as shown in Figure 1b.

To reduce the dosage of expensive noble Ag is of significance. The dispersion of active Ag species on appropriate supports is a simple and useful strategy. Here, we prepared bifunctional Ag/MgO for one pot synthesis of AcGly from NAG. A 26.2% yield was obtained under optimized conditions, as shown in Figure 1c. And the spent catalysts could be recycled and reused.

2. Materials and Methods

2.1 Materials

$AgNO_3$ (0.1009 mol/L) was purchased from Beijing Coastal Hongmeng Standard Material Technology Company. Na_2CO_3 (99.95%), MgO (AR, light), polyvinyl alcohol (PVA), ZrO_2 (99.99%), TiO_2 (99.8%), magnesium aluminum hydrotalcite (HT, 95%), γ-Al_2O_3 (99.99%), and anhydrous ethanol (99.9%) were purchased from Shanghai Titan Technology Company. Glycollic acid (GA, 99%), NAG (99%), formic acid (FA, 99%), acetic acid (AA, 99%), acetamide ($AcNH_2$, 98%) and AcGly (99%) were purchased from Adamas-beta (Shanghai, China). N-acetyl glucosaminic acid (NAGA) was prepared according to the literature [29]. All the chemicals were used without purification.

2.2. Catalyst Preparation

Several supported Ag catalysts were prepared by deposition-precipitation method. Taking Ag/MgO as an example, the typical preparation procedure is as follow. A desired amount of $AgNO_3$ solution (0.1009 mol/L) was added into 10 mL deionized water to form uniform solution A. Then PVA solution (10 mg/mL, 20 mL) and MgO suspension (0.5 g MgO, 20 mL deionized water) were mixed evenly to obtain stable suspension B. Under stirring, solution A was slowly added to suspension B drop by drop. After the addition, the mixture was stirred at room temperature for 1 h, followed by ultrasonic processing in an ice bath for 1 h. A Na_2CO_3 solution ($n(Na_2CO_3) = 2n (AgNO_3)$, 4 mL) was slowly added, and the mixture was stirred for 3 h at room temperature, aged for 1h and filtered. The solids were washed sequentially with 1 L of deionized water and 200 mL of absolute ethanol, then dried at 80 °C for 6 h. It was calcined in a muffle furnace at 550 °C for 2 h, with

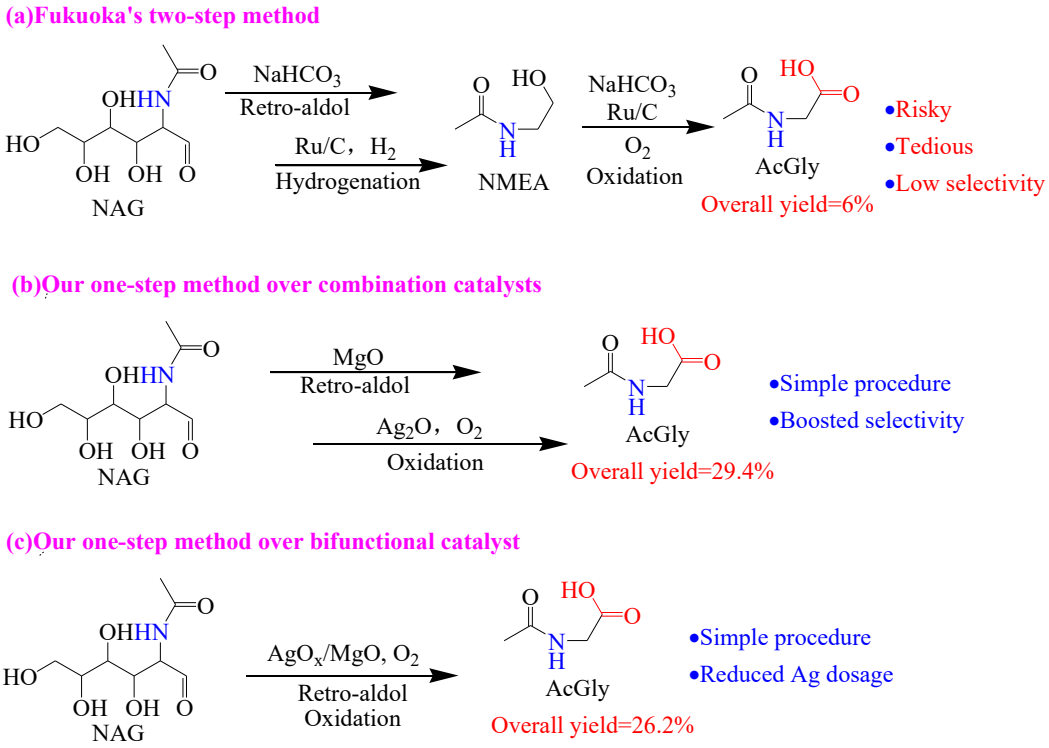

Figure 1. The synthesis of AcGly from NAG.

a heating rate of 5 °C /min. The as-prepared catalysts were denoted as Ag/support-X-Y. X represents theoretical loading (X%), while Y means preparation temperature, respectively.

2.3. Characterization Methods

Powder X-ray diffraction (XRD) patterns were recorded on a Shimadzu XRD-6100 diffractometer equipped with a Cu-Kα radiation source operating at 60 kV and 80 mA. Scans were performed over a 2θ range of 3° to 80° at a rate of 4°s-1. The X-ray photoelectron spectroscopy (XPS) measurements were conducted on a Thermo Scientific K-Alpha spectrometer using monochromatic Al Kα radiation (15 kV, 15 mA) to analyze the composition of Ag species. All binding energies were referenced to the adventitious C 1s peak at 284.8 eV. The actual loading of Ag was detected by inductively coupled plasma emission spectrometer (ICP, SPECTRO GENESIS), based on the standard curve of $AgNO_3$. Transmission electron microscope (TEM) pictures were collected on FEI-Talos F200S instrument.

2.4. Catalytic Activity Test and Product Analysis

The catalytic transformation of NAG to AcGly was carried out in an autoclave equipped with a stirrer. Typically, NAG (66.3 mg, 0.3 mmol), catalyst (5 mg), and water (5 mL) were added into the reactor. Pressurized O_2 (typically 0.3 MPa) was introduced into the reactor subsequently. Then the reactor was placed in an oil bath. After a desired time, the reaction was quenched by cold water and O_2 was released. Reaction liquid was collected by filtration, and used for HPLC analysis. The spent catalyst was washed with water, dried at 80 °C for 6 h, and used for stability testing.

The quantitative analysis of reactant and products was performed employing HPLC (Agilent 1260). The HPLC was equipped with an Aminex HPX- 87H Column (300×7.8 mm, 50 °C) and a PDA detector, where a 5 mM H_2SO_4 solution at a flow rate of 0.6 mL·min^{-1} was used as the mobile phase. NAG conversion and product yields were determined based on external standard curves.

3. Results and Discussion

3.1. Effect of Support

The effect of support type was investigated firstly. The acidic-basic properties have significant influence on AcGly formation. Both acid and base can catalyze retro- aldol reactions, but oxidation reaction usually requires basic medium. Therefore, basic supports might be favorable for our target reaction. Based on experimental results, the use of basic MgO and HT gave highest yields of AcGly (Table 1, entry 1-2), which supported our hypothesis. Trace AcGly (0.7%) was detected using Ag/Al_2O_3-6-450, maybe because that neutral Al_2O_3 bears no adequate acidic or basic sites. For comparison, additional basic MgO was added, resulting in a 12.5% yield of AcGly (Table 1, entry 5). The remarkable effect of MgO confirmed that NAG-AcGly transformation requires both retro-aldol and oxidation sites. The addition of MgO also enhanced the formation of GA and NAGA, implying that basic sites promote retro-aldol and oxidation reactions. No AcGly was detected when acidic supports (TiO_2 and ZrO_2) were used (Table 1, entry 6 and 8). Likewise, the addition of MgO also enhanced the transformation of NAG to AcGly (Table 1, entry 7 and 9), suggesting that MgO with alkalinity is an appropriate support.

3.2. Effect of Calcination Temperature

Then the effect of calcination temperature (250-650 °C) of Ag/MgO-6-Y catalysts was studied, and the results were shown in Figure 2. With the increase of temperature from 250 °C to 550 °C, AcGly yield increased from 10.5% to 14.7%, accompanying the slight increase of NAG conversion from 75.4% to 84.1%. After further

Table 1. The effect of support type on NAG conversion to AcGly.[a] ; [a]Reaction conditions: 0.3 mmol NAG, 5 mg catalyst, 5 mL H_2O，0.3 MPa O_2，130 ℃，2 h; [b]Adding 5 mg MgO

Entry	Catalyst	Conversion (%)	Yield (%)		
			AcGly	GA	NAGA
1	Ag/MgO-6-450	79.4	13.6	4.4	3.6
2	Ag/HT-6-450	59.2	7.6	3.9	5.2
3[b]	Ag/HT-6-450	75.5	14.5	1.4	1.1
4	Ag/Al_2O_3-6-450	22.5	0.7	0	0
5[b]	Ag/Al_2O_3-6-450	75.3	12.5	0.9	0.7
6	Ag/TiO_2-6-450	22.7	0	0	0
7[b]	Ag/TiO_2-6-450	92.2	16.4	5.8	0.9
8	Ag/ZrO_2-6-450	32.0	0	0	0
9[b]	Ag/ZrO_2-6-450	90.4	14.0	6.5	0.7

increasing temperature to 650 °C, AcGly yield was 14.9%, which was comparable to that using Ag/MgO-6-550. These results indicated that preparation temperature could affect catalytic activity. Ag/MgO-6-Y catalysts were further characterized by XPS, as shown in Figure 3 and Table 2. High temperatures could promote the reduction of Ag species, leading to the decrease of Ag^+/Ag^0 ratio. This can be explained by the decomposition of $AgNO_3$ or Ag_2O at high temperatures. After the temperature increases from 550 °C to 650 °C, the Ag^+/Ag^0 ratio increased, which can be explained by the re-oxidation of Ag at high temperature [38]. Possibly due to the cooperative roles of Ag^+ and Ag^0, the change of Ag^+/Ag^0 ratio to a suitable range contributed to the boosted yield of AcGly. XRD results (Figure 4) revealed the existence of MgO and $Mg(OH)_2$ in fresh Ag/MgO-6-250. The peaks belonging to $Mg(OH)_2$ disappeared after increasing preparing temperature. Therefore, basic MgO and $Mg(OH)_2$ can be converted into each other under certain conditions.

3.3. Effect of Ag Loading

Ag/MgO-X-550 catalysts with different Ag loading (2-10%) were prepared. The XRD patterns were employed to study catalyst structure. As shown in Figure 5, the peaks centered at 2θ = 38.2°, 44.2°, 64.5°, 77.5° were corresponding to (111), (200), (220) and (311) crystal planes of typical monoclinic Ag structure. With the increase of Ag loading, the intensity of the peaks (2θ=38.2°,44.2°, 64.5°and 77.5°) belonging to Ag (111), (200), (220) and (311) increased significantly, and these peaks became sharper, possibly resulting from the aggregation of Ag at higher loading. ICP results revealed that higher theoretical loading led to higher actual loading, as shown in Table 3.

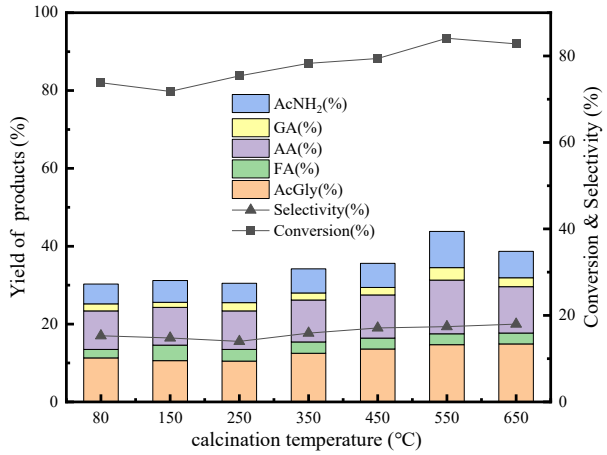

Figure 2. Influence of calcination temperature on catalytic conversion of NAG to AcGly. Reaction conditions：5 mg Ag/MgO-6-Y catalyst，0.3 mmol NAG，5 mL H_2O，0.3 MPa O_2，130 ℃，2 h.

The catalytic performance was tested and the results were shown in Figure 6. Comparable conversions of NAG (83.3-86.6%) were obtained, suggesting that Ag loading has no profound influence on NAG conversion. In consistent with these results, we also found that increasing Ag_2O amount could not promote the conversion in our previous study [37]. Therefore, both pure Ag_2O and supported Ag species could not catalyze NAG conversion alone. Maybe because the retro-aldol, oxidation or other reactions of NAG require basic medium. Ag loading has obvious effect on AcGly yield. When theoretical Ag loading was fixed as 2%, only 3.2% yield of AcGly was achieved, possibly due to lack of sufficient active Ag sites. The increase of Ag loading to 4% significantly enhanced AcGly formation, resulting in a 12.7% yield. Slight increase of AcGly yield was obtained by using larger amount of Ag loading. A highest AcGly yield of 16.5% was obtained over Ag/MgO-8-550.

The Ag/MgO-8-550 catalyst was characterized by TEM, as shown in Figure 7. The average size of Ag particle is about 100 nm. The

Table 3. ICP analysis of Ag/MgO-X-550 catalysts.

Theoretical loading of Ag (%)	Actual loading of Ag (%)
2	1.6
4	1.7
6	1.8
8	2.0
10	3.1

Table 2. Binding energies of Ag^0 and Ag^+ and the ratio of Ag^+/Ag^0 from XPS spectra.

Catalyst	Ag3d 3/2		Ag3d 5/2		Ag^+/Ag^0
	Ag^0 (eV)	Ag^+ (eV)	Ag^0 (eV)	Ag^+ (eV)	
Ag/MgO-6-150	374.82	373.98	371.19	368.02	4.43
Ag/MgO-6-250	374.59	374.05	371.51	368.06	4.39
Ag/MgO-6-350	374.51	373.73	371.41	367.77	2.85
Ag/MgO-6-450	374.65	374.25	371.60	368.31	0.99
Ag/MgO-6-550	374.74	373.7	371.13	367.17	0.39
Ag/MgO-6-650	374.35	373.9	371.34	367.91	3.2

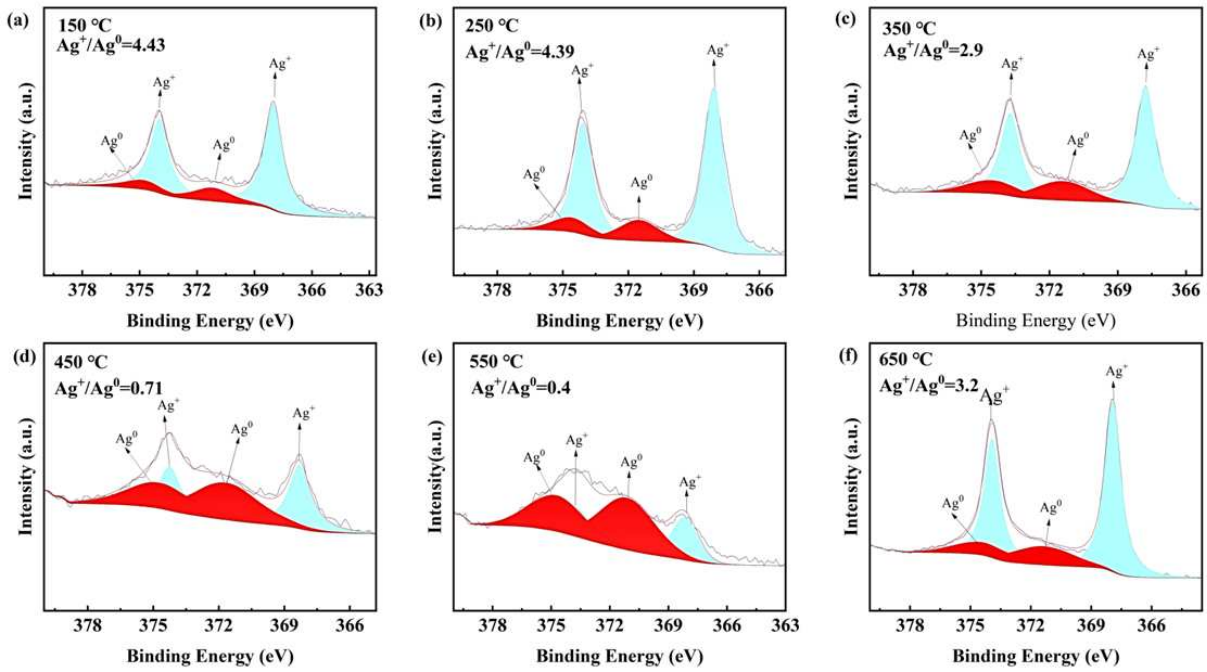

Figure 3. XPS spectra of Ag/MgO-6-Y catalysts.

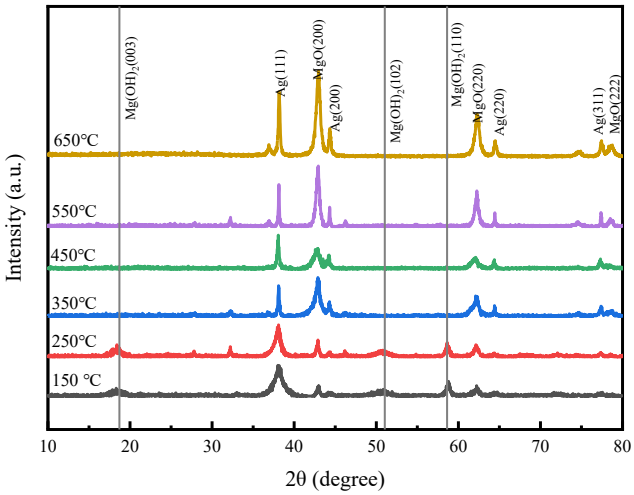

Figure 4. XRD patterns of Ag/MgO-6-Y catalysts.

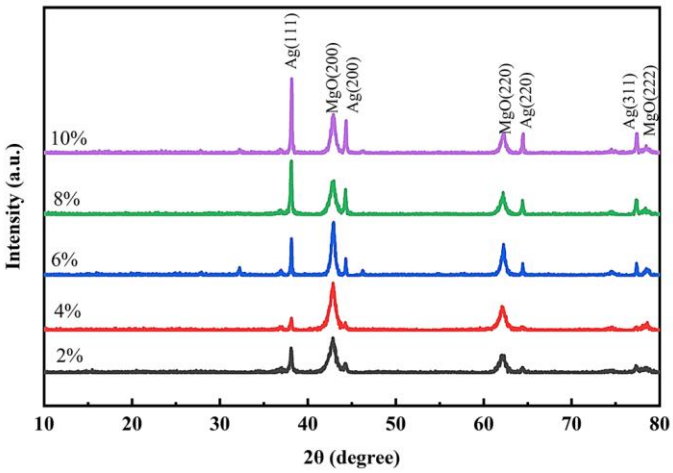

Figure 5. XRD patterns of Ag/MgO-X-550 catalysts.

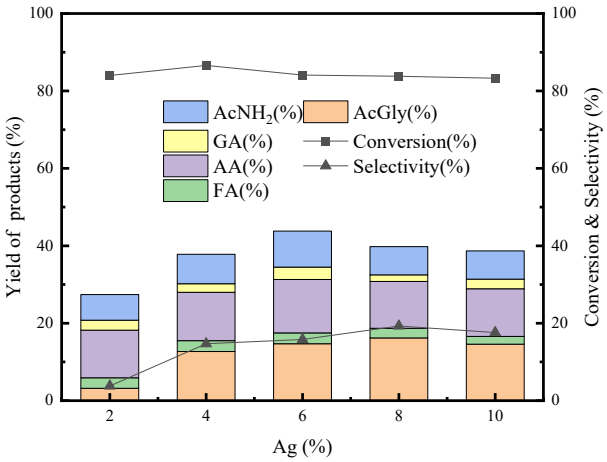

Figure 6. Effect of Ag loading on catalytic conversion of NAG to AcGly. Reaction conditions：5 mg Ag/MgO-X-550 catalyst，0.3 mmol NAG，5 mL H_2O，0.3 MPa O_2，130 ℃，2 h.

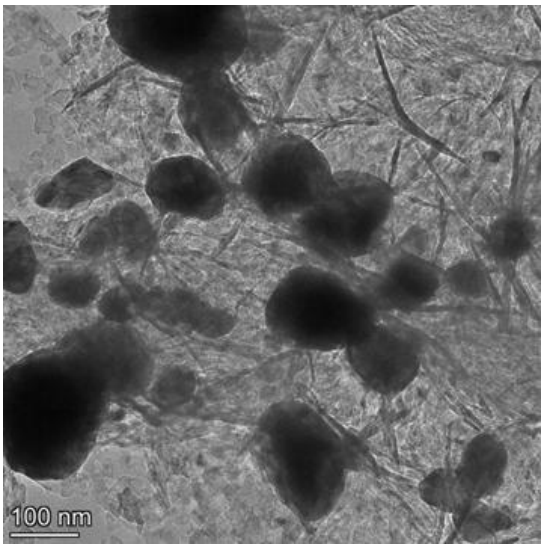

Figure 7. TEM image of Ag/MgO-8-550.

relatively large size might associate with the limited surface area of MgO.

3.4. Effect of Reaction Temperature

The reaction conditions for one pot conversion of NAG to AcGly were meticulously studied. As shown in Figure 8a, reaction temperature has obvious effect. When reaction was conducted at low temperatures, both NAG conversion and AcGly yield were low. For example, only 35.7% conversion of NAG and 3.3% yield of AcGly were obtained at 80 °C for 2 h, and the selectivity of AcGly was 9.9%. A trace amount of NAGA (0.5%) was detected, implying the occurrence of direct oxidation of NAG. With the increase of temperature, NAG conversion monotonically increased. Meanwhile, AcGly yield increased firstly and the maximum yield of 16.5% was obtained at 130 °C. Higher temperature than 130 °C led to slight decrease of AcGly yield, maybe because of instability of AcGly at high temperature. High temperature favored the formation of FA, AA, $AcNH_2$ and GA, probably because oxidation reactions were enhanced at high temperature. Interestingly, when reaction temperature was 130-150 °C, no NAGA was detected, which is consistent with previous study employing MgO and Ag_2O, implying that NAGA was not stable [37].

3.5. The Influence of Oxygen Pressure

NAG-AcGly transformation involves C-C cleavage and oxidation reaction. The effect of oxidant (O_2 pressure) was investigated, and the results were shown in Figure 8b. When O_2 pressure increased from 0.2 MPa to 0.3 MPa, AcGly yield increased from 12.6% to 16.2%. Further increasing O_2 pressure led to slight decrease of AcGly. 12.7% yield of AcGly was obtained at 1.0 MPa O_2, and NAG conversion also decreased slightly to 78.2%. Therefore, high O_2 pressure is not required in our system.

3.6. The Impact of Catalyst Dosage

The effect of catalyst dosage was studied. As shown in Figure 8c, in presence of 2.5 mg catalyst, 69.5% NAG conversion and only 9.7% AcGly yield were obtained, indicating that no enough active sites were provided. The addition of 5 mg catalyst afforded boosted NAG conversion (83.8%) and AcGly yield (16.2%). By further increasing catalyst amount to 10 mg, slight increase of NAG conversion and comparable AcGly yield were obtained. Too much catalyst led to slight decrease of AcGly yield. Excess active sites might cause some base-catalyzed or Ag-catalyzed side reactions. Thus, the yields of several side

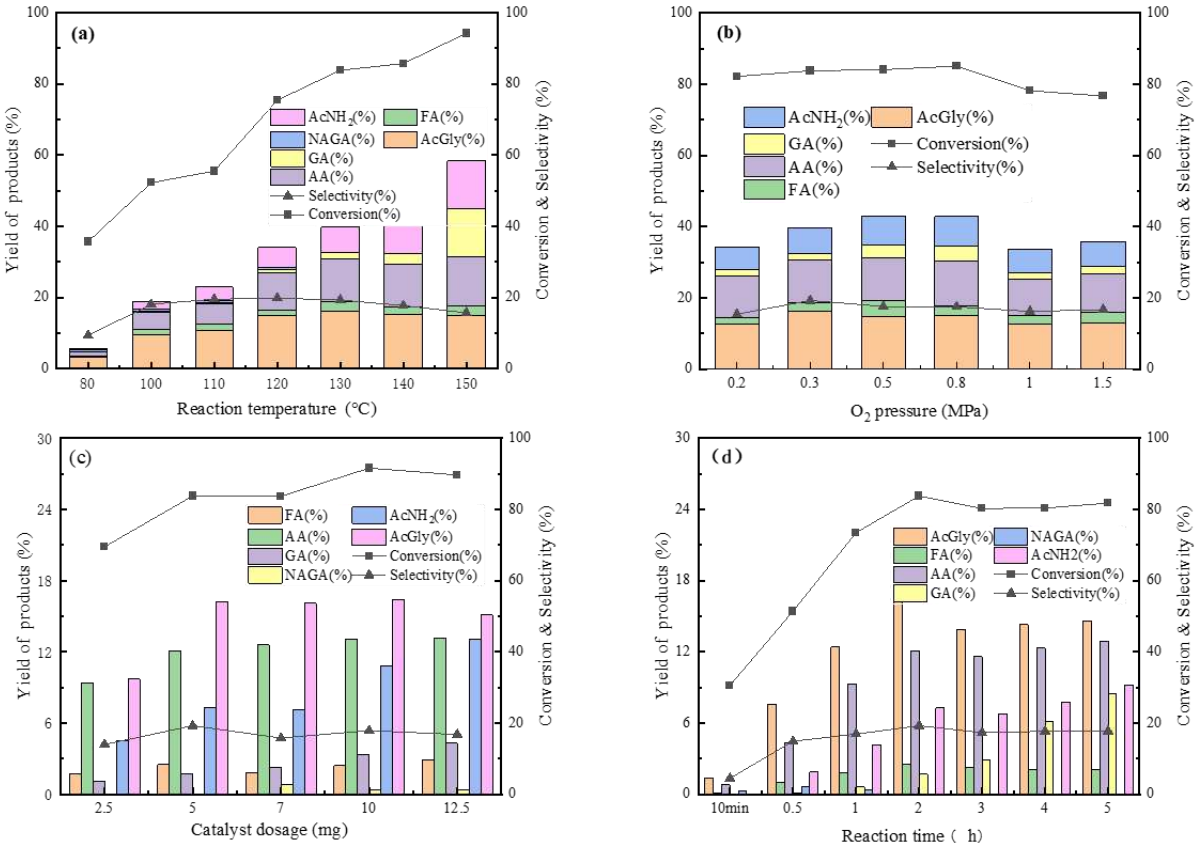

Figure 8. The effect of (a) reaction temperature, (b) O_2 pressure, (c) catalyst dosage, and (d) reaction time on NAG conversion. Reaction conditions: 0.3 mmol of NAG, 5 mL of H_2O. (a) 5 mg of Ag/MgO-8-550 catalyst, 0.3 MPa O_2, 2 h; (b) 130 °C, 2 h, 5 mg of Ag/MgO-8-550 catalyst; (c) 130 °C, 2 h, 0.3 MPa O_2; (d) 5 mg of Ag/MgO-8-550 catalyst, 2 h, 0.3 MPa O_2.

products, including AA, $AcNH_2$ and GA, increased after increasing catalyst amount.

3.7. Effect of Reaction Time

Then we screened AcGly production as a function of time using 5 mg catalyst, as shown in Figure 8d. After reaction for 10 min, 30.6% NAG has been converted, but the yield of AcGly was as low as 1.4%. The selectivity of AcGly was 4.5%. Meanwhile, trace amount of FA, AA and NAGA was detected in yields of 0.1%, 0.8% and 0.3%, respectively. NAG conversion increased to 51.4% for 0.5 h, while AcGly yield was 7.6%. The selectivity of AcGly significantly increased to 14.5%. A highest 16.2% yield of AcGly with 19.3% selectivity was obtained for 2 h. As proposed in our previous study, NAGA was a possible intermediate during AcGly formation [37]. In the early stage (reaction time $\leqslant$1 h), trace amount of NAGA (0.3-0.6%) was detected. When reaction time was prolonged from 1 h to 2 h, NAGA disappeared, which can be explained by the conversion of NAGA to AcGly and other products. Long reaction time favored the generation of AA, $AcNH_2$ and GA.

3.8. Effect of NAG Concentration

The effect of NAG concentration was investigated (Figure 9). Generally, there is a seesaw relationship between NAG concentration and AcGly selectivity. When NAG concentration was fixed as 0.06 mol/L, a 16.2% AcGly yield and an 83.8% conversion were obtained by optimizing catalyst preparation parameters and reaction parameters. The increase of NAG concentration from 0.06 mol/L to 0.12 mol/L led to sharp decrease of AcGly yield from 16.2% to 8.6%, which can be explained by insufficient active sites. On the other hand, when NAG concentration decreased from 0.06 mol/L to 0.01 mol/L, a highest 26.2% AcGly yield with 96.1% conversion was obtained. As shown in Table 4, some typical results about AcGly production from NAG were summarized. The obtained AcGly yield using Ag/MgO was comparable to that over MgO and Ag_2O [37], and much higher than that employing Ru/C and $NaHCO_3$ in a two-step procedure [29]. Meanwhile, the dosage of noble meta reduced significantly compared to MgO-Ag_2O system , as supported by higher TOF value.

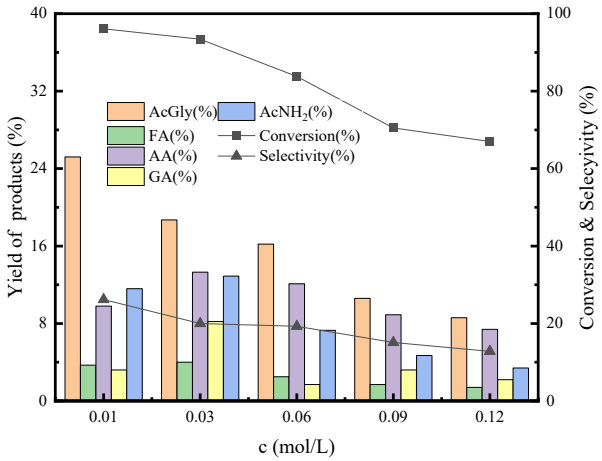

Figure 9. Effect of NAG concentration on NAG conversion to AcGly. Reaction conditions: 5 mg Ag/MgO-8-550 catalyst, 5 mL H_2O, 130 ℃, 2 h, 0.3 MPa O_2.

Table 4. Catalytic conversion of NAG to AcGly. (TOF: Turn over Frequency)

Entry	Catalysts	Reaction conditions	Conversion (%)	AcGly yield (%)	TOF (h^{-1})	Ref.
1	5%Ru/C + $NaHCO_3$	1st step : 2 mmol NAG, 200 mg Ru/C, 2 mmol $NaHCO_3$, 40 mL H_2O, 4 MPa H_2, 120 °C, 1 h. Temperature was increased to 120 °C at p(H_2) of 0.1 MPa, and p(H_2) was then increased to 4 MPa. 2nd step : 2 mmol NMEA, 200 mg Ru/C, 2 mmol $NaHCO_3$, 40 mL H_2O, 1 MPa O_2, 120 °C, 1 h.	1st step: >99.0%; 2nd step: 97%.	1st step: 29%; 2nd step: 21%; Overall yield: 6%.	1st step: 5.8; 2nd step: 4.2.	29
2	MgO+Ag_2O	0.05 mmol NAG, 0.5 mmol MgO, 0.05 mmol Ag_2O, 5 mL H_2O, 0.3 MPa O_2, 130 °C, 2 h.	99.0%	29.4%	0.15	37
3	Ag/MgO-8-550	0.05mmol NAG, 20 mg Ag/MgO-8-550, 5 mL H_2O, 0.3 MPa O_2, 130 °C, 2 h.	96.1%	26.2%	1.7	This work

3.9. Catalyst Stability

Last but not least, the stability of the catalyst under reaction conditions was investigated (Figure 10). After 3 catalytic runs, NAG conversion has no obvious changes and remained at about 80%, while AcGly yield gradually decreased to 11.2%. There are two possible reasons for deactivation. Firstly, there is inevitable mass loss of catalyst during recycling experiment. Secondly, XRD results of spent catalyst indicated that the structure of MgO was destroyed during reaction, possibly due to acidic products like AcGly. These results implied that partially recyclable bi-functional Ag/MgO catalysts were successfully prepared. Future efforts should focus on elucidating the cause of the observed decline in AcGly yield and developing strategies to enhance the catalyst's long-term stability for further improvements.

4. Conclusion

To reduce the dosage of precious metal Ag, supported catalysts were prepared by simple deposition-precipitation method. The alkaline supports of Ag catalysts favored one pot conversion of NAG to AcGly without requiring other additives. In contrast, the use of acidic or neutral supports requires additional base catalysts. Ag/MgO exhibited best activity for AcGly formation. By altering the preparation temperature, the ratio of Ag^+/Ag^0 can be adjusted. And the activity of Ag0 was found to be higher than Ag^+. The yield of AcGly decreased slightly after 3 catalytic runs. An AcGly yield of 26.2% was obtained under optimized conditions (5 mL 0.01 mol/L NAG aqueous solution, 5 mg Ag/MgO-8-550, 130 ℃, 2 h, 0.3 MPa O_2). This yield was comparable to that using Ag_2O and MgO. Meanwhile, the dosage of Ag reduced remarkably.

Acknowledgment

The authors gratefully acknowledge the support of the National Natural Science Foundation of China (22408032), the Science and Technology Research Program of Chongqing Municipal Education Commission (KJQN202200844), and the Chongqing College Students' Innovation and Entrepreneurship Training Program (S202411799022).

CRedit Author Statement

Author Contributions: D. Qi: investigation, formal analysis, writing original draft; Q. Cao: investigation, formal analysis, writing original draft and revising manuscript; C. Huang: investigation, formal analysis; X. Qi: investigation, formal analysis; C. Wang: investigation; J. Dai: conceptualization, project administration, funding acquisition & editing. The authors have read and agreed to the published version of the manuscript.

References

[1] Deng, W., Feng, Y., Fu, J., Guo, H., Guo, Y., Han, B., Jiang, Z., Kong, L., Li, C., Liu, H. (2023). Catalytic conversion of lignocellulosic biomass into chemicals and fuels. *Green Energy & Environment*, 8 (1), 10-114. DOI: 10.1016/j.gee.2022.07.003.

[2] Du, Z., Yang, D., Cao, Q., Dai, J., Yang, R., Gu, X., Li, F. (2023). Recent advances in catalytic synthesis of 2,5-furandimethanol from 5-hydroxymethylfurfural and carbohydrates. *Bioresources and Bioprocessing*, 10 (1), 52. DOI: 10.1186/s40643-023-00676-x.

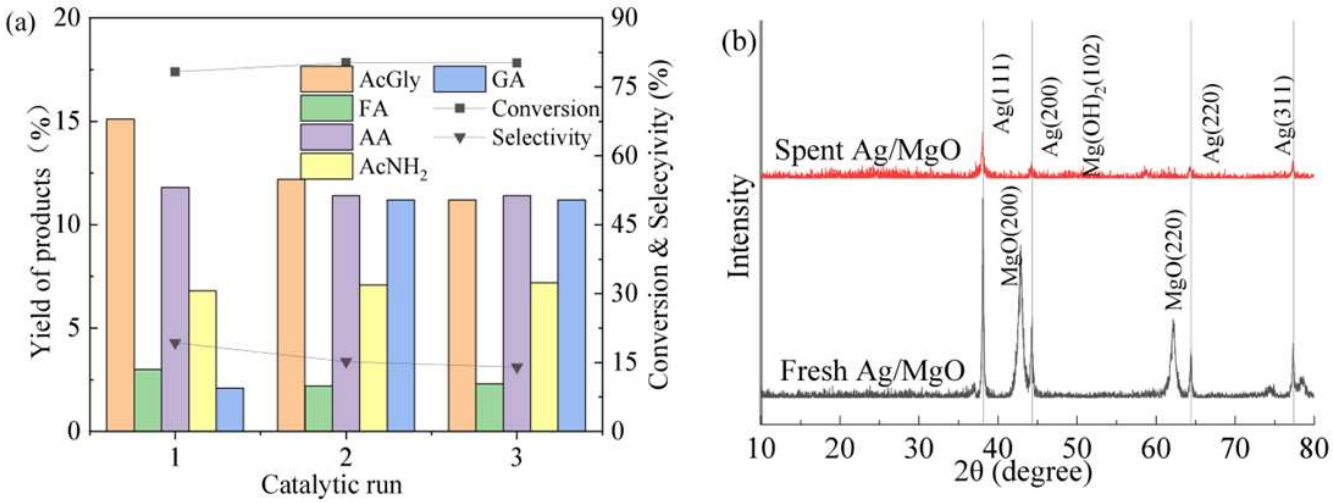

Figure 10. Evaluation of catalyst stability. (a) Recyclability of Ag/MgO-8-550 catalyst for catalytic conversion of NAG to AcGly. Reaction conditions: 0.3 mmol of NAG, 5 mg of Ag/MgO-8-550, 5 mL of H_2O, 0.3 MPa O_2, 130 °C, 2 h. (b) XRD patterns of fresh and spent Ag/MgO-8-550.

[3] Chen, X., Song, S., Li, H., Gözaydın, G.K., Yan, N. (2021). Expanding the boundary of biorefinery: organonitrogen chemicals from biomass. *Accounts of Chemical Research*, 54 (7), 1711-1722. DOI: 10.1021/acs.accounts.0c00842.

[4] Dai, J., Li, F., Fu, X. (2020). Towards shell biorefinery: advances in chemical-catalytic conversion of chitin biomass to organonitrogen chemicals. *ChemSusChem*, 13 (24), 6498-6508. DOI: 10.1002/cssc.202001955.

[5] Hulsey, M.J., Yang, H.Y., Yan, N. (2018). Sustainable routes for the synthesis of renewable heteroatom-containing chemicals. *ACS Sustainable Chemistry & Engineering*, 6 (5), 5694-5707. DOI: 10.1021/acssuschemeng.8b00612.

[6] Qaseem, M.F., Shaheen, H., Wu, A.-M. (2021). Cell wall hemicellulose for sustainable industrial utilization. *Renewable and Sustainable Energy Reviews*, 144, 110996. DOI: 10.1016/j.rser.2021.110996.

[7] Shi, X., Ye, X., Zhong, H., Wang, T., Jin, F. (2021). Sustainable nitrogen-containing chemicals and materials from natural marine resources chitin and microalgae. *Molecular Catalysis*, 505, 111517. DOI: 10.1016/j.mcat.2021.111517.

[8] Li, X., Xu, Y., Alorku, K., Wang, J., Ma, L. (2023). A review of lignin-first reductive catalytic fractionation of lignocellulose. *Molecular Catalysis*, 550, 113551. DOI: 10.1016/j.mcat.2023.113551.

[9] Yan, N., Chen, X. (2015). Don't waste seafood waste. *Nature*, 524 (7564), 155-157. DOI: 10.1038/524155a.

[10] Chen, X., Yang, H., Yan, N. (2016). Shell Biorefinery: Dream or Reality? *Chemistry-a European Journal*, 22 (38), 13402. DOI: 10.1002/chem.201602389.

[11] Xu, B., Dai, J., Du, Z., Li, F., Liu, H., Gu, X., Wang, X., Li, N., Zhao, J. (2023). Catalytic conversion of biomass-derived compounds to various amino acids: Status and perspectives. *Frontiers of Chemical Science and Engineering*, 17 (7), 817-829. DOI: 10.1007/s11705-022-2254-z.

[12] Kobayashi, H., Sagawa, T., Fukuoka, A. (2023). Catalytic conversion of chitin as a nitrogen-containing biomass. *Chemical Communications*, 59 (42), 6301-6313. DOI: 10.1039/D3CC00902E.

[13] Rogers, R.D., Kerton, F.M. (2022). Marine-based green chemistry. *Green Chemistry*, 24 (6), 2265-2266. DOI: 10.1039/D2GC90018A.

[14] Xing, A., Secundo, F., Xue, C., Hu, Y., Mao, X. (2024). Green and Efficient Preparation of Nano-chitin for Enzymatic Preparation of N-Acetylchitooligosaccharides. *ACS Sustainable Resource Management*, 1 (1), 88-96. DOI: 10.1021/acssusresmgt.3c00044.

[15] Gözaydın, G.K., Sun, Q., Oh, M., Lee, S., Choi, M., Liu, Y., Yan, N. (2023). Chitin hydrolysis using zeolites in lithium bromide molten salt hydrate. *ACS Sustainable Chemistry & Engineering*, 11 (6), 2511-2519. DOI: 10.1021/acssuschemeng.2c06675.

[16] Cao, S., Liu, Y., Shi, L., Zhu, W., Wang, H. (2022). N-Acetylglucosamine as a platform chemical produced from renewable resources: opportunity, challenge, and future prospects. *Green Chemistry*, 24 (2), 493-509. DOI: 10.1039/D1GC03725K.

[17] Ji, X., Kou, J., Gozaydin, G., Chen, X. (2024). Boosting 3-acetamido-5-acetylfuran production from N-acetyl-D-glucosamine in γ-valerolactone by a dissolution-dehydration effect. *Applied Catalysis B: Environmental*, 342, 123379. DOI: 10.1016/j.apcatb.2023.123379.

[18] Wu, C., Zhu, X., Zang, H., Liu, Z., Zhu, X., Chang, Y. (2024). Efficient conversion of N-acetyl-D-glucosamine into organonitrogen compound 3-acetamido-5-acetylfuran via a novel tandem coordination-catalysis process catalyzed by WCl6-based Brønsted-Lewis acidic ionic liquid. *Molecular Catalysis*, 566, 114404. DOI: 10.1016/j.mcat.2024.114404.

[19] Yamazaki, K., Hiyoshi, N., Yamaguchi, A. (2023). Conversion of N-Acetylglucosamine to 3-Acetamido-5-Acetylfuran over Al-Exchanged Montmorillonite. *ChemistryOpen*, 12 (12), e202300148. DOI: 10.1002/open.202300148.

[20] Chen, K., Wu, C., Wang, C., Zhang, A., Cao, F., Ouyang, P. (2021). Chemo-enzymatic protocol converts chitin into a nitrogen-containing furan derivative, 3-acetamido-5-acetylfuran. *Molecular Catalysis*, 516, 112001. DOI: 10.1016/j.mcat.2021.112001.

[21] Dai, J., Cao, Q., Yang, D., Chen, G., Du, Z., Wang, S., Li, F. (2025). 3-Acetamido-5-acetylfuran: An emerging renewable nitrogen-containing platform compound. *Chinese Journal of Chemical Engineering*, 78, 263-272. DOI: 10.1016/j.cjche.2024.10.029.

[22] Liu, Y., Stähler, C., Murphy, J.N., Furlong, B.J., Kerton, F.M. (2017). Formation of a Renewable Amine and an Alcohol via Transformations of 3-Acetamido-5-acetylfuran. *ACS Sustainable Chemistry & Engineering*, 5 (6), 4916. DOI: 10.1021/acssuschemeng.7b00323.

[23] Pham, T.T., Gözaydın, G., Söhnel, T., Yan, N., Sperry, J. (2019). Oxidative Ring-Expansion of a Chitin-Derived Platform Enables Access to Unexplored 2-Amino Sugar Chemical Space. *European Journal of Organic Chemistry*, 2019 (6), 1355-1360. DOI: 10.1002/ejoc.201801683.

[24] Pereira, J.G., Ravasco, J.M., Vale, J.R., Queda, F., Gomes, R.F. (2022). A direct Diels–Alder reaction of chitin derived 3-acetamido-5-acetylfuran. *Green Chemistry*, 24 (18), 7131-7136. DOI: 10.1039/D2GC00253A.

[25] Sadiq, A.D., Chen, X., Yan, N., Sperry, J. (2018). Towards the shell biorefinery: sustainable synthesis of the anticancer alkaloid proximicin A from chitin. *ChemSusChem*, 11 (3), 532-535. DOI: 10.1002/cssc.201702356.

[26] Dai, J.H., Gozaydin, G., Hu, C.W., Yan, N. (2019). Catalytic conversion of chitosan to glucosaminic acid by tandem hydrolysis and oxidation. *ACS Sustainable Chemistry & Engineering*, 7 (14), 12399-12407. DOI: 10.1021/acssuschemeng.9b01912.

[27] Dai, J., Cao, Q., Du, Z., Yang, R., Yang, D., Li, F., Gu, X. (2023). Facile synthesis of N-acetylglycine from chitin-derived N-acetylmonoethanolamine. *Catalysis Communications*, 185, 106812. DOI: 10.1016/j.catcom.2023.106812.

[28] Ohmi, Y., Nishimura, S., Ebitani, K. (2013). Synthesis of alpha-amino acids from glucosamine-HCl and its derivatives by aerobic oxidation in water catalyzed by Au nanoparticles on basic supports. *ChemSusChem*, 6 (12), 2259-2262. DOI: 10.1002/cssc.201300303.

[29] Techikawara, K., Kobayashi, H., Fukuoka, A. (2018). Conversion of N-acetylglucosamine to protected amino acid over Ru/C catalyst. *ACS Sustainable Chemistry & Engineering*, 6 (9), 12411-12418. DOI: 10.1021/acssuschemeng.8b02951.

[30] Kobayashi, H., Techikawara, K., Fukuoka, A. (2017). Hydrolytic hydrogenation of chitin to amino sugar alcohol. *Green Chemistry*, 19 (14), 3350-3356. DOI: 10.1039/c7gc01063j.

[31] Lin, C., Xu, L., Zhuang, Y., Ma, P., Wu, H., Gan, H., Cao, F., Wei, P. (2024). Oxy-vacancy Mo-acetylacetone catalyzes N-acetylglucosamine to co-produce furan and pyrrole compounds. *Chemical Engineering Science*, 121099. DOI: 10.1016/j.ces.2024.121099.

[32] Harburn, J.J., Rath, N.P., Spilling, C.D. (2005). Efficient synthesis of tyrosine-derived marine sponge metabolites via acylation of amines with a coumarin. *The Journal of Organic Chemistry*, 70 (16), 6398-6403. DOI: 10.1021/jo050846r.

[33] Jiang, F., Chen, K.-X., Xiang, J.-M., Shen, Y.-C. (2024). An Enzymatic Method to Obtain Enantiopure 3-Pyridyl and Substituted Phenyl Alanine. *Chirality*, 36 (11), e70000. DOI: 10.1002/chir.70000.

[34] Li, R., Dong, G. (2020). Structurally modified norbornenes: a key factor to modulate reaction selectivity in the palladium/norbornene cooperative catalysis. *Journal of the American Chemical Society*, 142 (42), 17859-17875. DOI: 10.1021/jacs.0c09193.

[35] Meng, G., Lam, N.Y., Lucas, E.L., Saint-Denis, T.G., Verma, P., Chekshin, N., Yu, J.-Q. (2020). Achieving site-selectivity for C–H activation processes based on distance and geometry: a carpenter's approach. *Journal of the American Chemical Society*, 142 (24), 10571-10591. DOI: 10.1021/jacs.0c04074.

[36] Venkatesan, G. (2021). Third-order nonlinear and linear optical properties of n-acetyl glycine hydrochloride crystal for optical applications. *Journal of Optics*, 50 (2), 169-176. DOI: 10.1007/s12596-021-00696-w.

[37] Cao, Q., Dai, J., Du, Z., Chen, G., Li, F., Qi, T., Wang, R., Wang, W., Zhao, J., Huang, C. (2025). One-pot green synthesis of N-acetylglycine from renewable N-acetyl glucosamine. *Organic & Biomolecular Chemistry*, 23 (21), 5126-5132. DOI: 10.1039/D5OB00577A.

[38] Song, Y., Xu, M., Li, Z., He, L., Hu, M., He, L., Zhang, Z., Du, M. (2020). Ultrasensitive detection of bisphenol A under diverse environments with an electrochemical aptasensor based on multicomponent AgMo heteronanostructure. *Sensors and Actuators B: Chemical*, 321, 128527. DOI: 10.1016/j.snb.2020.128527.